Thermomagnetic Effects in Superconductors

P. R. SOLOMON AND F. A. OTTER, JR.
United Aircraft Research Laboratories, East Hartford, Connecticut
(Received 1 June 1967)

Transport properties of superconductors in the mixed state and the intermediate state are discussed. The paper outlines a phenomenological model for the thermomagnetic effects occurring when vortices are free to move. These effects involve the entropy transported by moving vortices. We have described the measurement of two effects which are abnormally large in a superconductor, the Ettingshausen effect and the Nernst effect. Both effects have been measured as functions of magnetic field and temperature in a type-II alloy (In+40 at.% Pb), and the Ettingshausen effect has been measured in a type-I alloy (Sn+0.05 at.% In). The values of transported entropy per cm of flux line per flux quantum computed from these measurements are compared with existing theories. For both type-I and type-II superconductors, the theories agree roughly with the measurements at low temperatures but fail to agree near T_c.

I. INTRODUCTION

IT has been generally assumed that all thermoelectric effects disappear in the superconducting state.[1] Recently, however, there has been speculation that thermoelectric effects may occur in a superconductor in the mixed or intermediate state.[2] Several such thermomagnetic effects have now been observed.[3–5] They occur only in the presence of quantized flux line (vortex) motion. Vortex motion is believed to exist when a type-II superconductor exhibits electrical resistance.[6] Recent experiments have shown that under certain circumstances vortex motion exists when a type-I superconductor in the intermediate state exhibits electrical resistance.[7–9] The thermomagnetic effects occur because moving vortices can carry entropy, and thermal gradients can exert forces on vortices.

Section II of this paper is a discussion of the mechanism for these effects. The experimental details of the measurement of two of them, the Nernst effect and the Ettingshausen effect, appear in Secs. III and IV. Section V contains the results of the measurements of both effects in a type-II superconductor and a comparison of the results with recently proposed theories[10,11] and with the results of calorimetric measurements[12] of the total entropy associated with a vortex. Section VI contains the results of measurements of the Ettingshausen effect in a type-I superconductor and a comparison of the results with a simple model. Section VII summarizes the results.

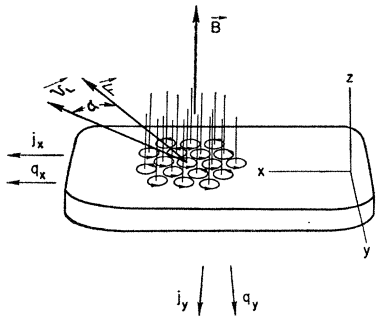

FIG. 1. Sample geometry.

II. GENERAL DISCUSSION OF THERMOMAGNETIC EFFECTS

Consider an isotropic material situated in a magnetic field B pointing along the positive z axis as shown in

[1] See, for example, D. Shoenberg, *Superconductivity* (Cambridge University Press, New York, 1960).

[2] Yu. V. Sharvin, Zh. Eksperim. i Teor. Fiz. Pis'ma v Redaktsiyu **2**, 287 (1965) [English transl.: Soviet Phys.—JETP Letters **2**, 183 (1965)]; and J. Volger, in *Quantum Fluids*, edited by D. F. Brewer (North-Holland Publishing Company, Amsterdam, 1966), p. 132.

[3] A. T. Fiory and B. Serin, Phys. Rev. Letters **16**, 308 (1966).

[4] F. A. Otter, Jr., and P. R. Solomon, Phys. Rev. Letters **16**, 681 (1966); in *Proceedings of the Tenth International Conference on Low-Temperature Physics, Moscow, 1966* (Proizvodstrenno-Izdatel'skii Kombinat, VINITI, Moscow, USSR, 1967); P. R. Solomon, F. A. Otter, Jr., G. B. Yntema, and J. B. Burnham, Bull. Am. Phys. Soc. **11**, 480 (1966); and P. R. Solomon, in *Proceedings of the Tenth International Conference on Low-Temperature Physics, Moscow, 1966* (Proizvodstrenno-Izdatel'skii Kombinat, VINITI, Moscow, USSR, 1967).

[5] J. Lowell, J. S. Muñoz, and J. Sousa, Phys. Letters **24A**, 376 (1967).

[6] For a discussion of electrical resistance in type-II superconductors, see, for example: Y. B. Kim, C. F. Hempstead, and A. R. Strnad, Phys. Rev. **139**, A1163 (1965); C. F. Hempstead and Y. B. Kim, Phys. Rev. Letters **12**, 145 (1964); A. R. Strnad, C. F. Hempstead, and Y. B. Kim, *ibid.* **13**, 694 (1964); J. Volger, F. A. Staas, and A. G. van Vijfeijken, Phys. Letters **9**, 303 (1964); W. F. Druyvesteyn and J. Volger, Philips Res. Rept. **19**, 359 (1964); P. H. Borcherds, C. E. Gough, W. F. Vinen, and A. C. Warren, Phil. Mag. **10**, 349 (1964). Experimental verification of flux flow in a type-II superconductor has been obtained by Ivar Giaever, Phys. Rev. Letters **15**, 825 (1965).

[7] P. R. Solomon, Phys. Rev. Letters **16**, 50 (1966); in *Proceedings of the Tenth International Conference on Low-Temperature Physics, Moscow, 1966* (Proizvodstrenno-Izdatel'skii Kombinat, VINITI, Moscow, USSR, 1967).

[8] G. J. Van Gurp, Phys. Letters **24A**, 528 (1967).

[9] Additional evidence for flux flow in type-I superconductors is provided by the work of B. S. Chandrasekhar, J. J. Dinewitz, and D. E. Farrell [Phys. Letters **20**, 321 (1966)] and the work of J. Pearl [Phys. Rev. Letters **16**, 99 (1966)], although the results of Pearl are not conclusive proof of vortex motion as shown by P. P. M. Meincke [Phys. Rev. Letters **17**, 390 (1966)]. Experimental evidence for the motion of laminar domains provided by Sharvin (Ref. 2) has recently been questioned by B.S. Chandrasekhar, D. E. Farrell, and S. Huang [Phys. Rev. Letters **18**, 43 (1967)] and by B. L. Brandt and R. D. Parks [Phys. Rev. Letters **19**, 163 (1967)].

[10] M. J. Stephen, Phys. Rev. Letters **16**, 801 (1966).

[11] A. G. van Vijfeijken, Phys. Letters **23**, 65 (1966).

[12] F. A. Otter, Jr., and G. B. Yntema, Bull. Am. Phys. Soc. **11**, 107 (1966); Ann. Acad. Sci. Fennicae **210**, 98 (1966).

Fig. 1. For simplicity let the flows (electrical current density $\mathbf{j}$ and heat current density $\mathbf{q}$) and the driving forces (the gradients of electrochemical potential for electrons μ and temperature T) have only x and y components.

We first review the thermomagnetic effects in a normal conductor.[13] The flows may be conveniently related to the driving forces by the following expression:

$$\begin{pmatrix} -j_x/e \\ -j_y/e \\ q_x \\ q_y \end{pmatrix} = L(B) \begin{pmatrix} (1/T)\nabla_x\mu \\ (1/T)\nabla_y\mu \\ \nabla_x(1/T) \\ \nabla_y(1/T) \end{pmatrix}, \quad (1)$$

where e is the charge of the current carrier and $L(B)$ is a 4×4 matrix. The Onsager relations[14] require that $L_{ij}(B)=L_{ji}(-B)$. The thermomagnetic coefficients are defined in terms of the currents and driving forces. For example, the Nernst coefficient is $-\nabla_y\mu/(eB\nabla_xT)$ under the conditions $j_x=j_y=q_y=0$ (i.e., the Nernst effect is an electrochemical potential gradient in the y direction produced by a temperature gradient in the x direction), and the Ettingshausen coefficient is ∇_yT/Bj_x under the conditions $j_y=q_y=\nabla_xT=0$ (i.e., the Ettingshausen effect is a temperature gradient in the y direction produced by an electrical current in the x direction).

The relation between currents and driving forces in a superconductor is more complicated. We outline a simple phenomenological model for the thermomagnetic effects. Its purpose is to review the properties of the flux-flow state and define a useful set of parameters. We start with the acceleration equation for the superfluid electrons[15,16]:

$$\partial\mathbf{v}_s(r)/\partial t=-\nabla\mu(r)/m-(e/mc)\partial\mathbf{A}(r)/\partial t, \quad (2)$$

where $\mathbf{v}_s(r)$ is the average velocity of superfluid electrons at point r, $\mathbf{A}(r)$ is the vector potential, m is the electron mass, and $\mu(r)$ is the electrochemical potential per electron. $\mu(r)$ can be written as $\mu_0(r,T)+(\frac{1}{2})mv_s(r)^2+eV(r)$, where $V(r)$ is the electrical potential. In the steady state (no flux flow; $\partial\mathbf{v}_s/\partial t=\partial\mathbf{A}/\partial t=0$), Eq. (2) requires that $\nabla\mu$ be zero. Therefore, the electrical resistance, the thermoelectric power, the Hall coefficient, and the Nernst coefficient which are proportional to some component of $\nabla\mu$ must all be zero.[17] The Peltier coefficient and the Ettingshausen coefficient must also be zero, since otherwise a temperature gradient developed by a persistent ring current could in principle drive a heat engine in violation of conservation of energy.

When a superconductor is in the mixed or intermediate state, the situation must be quite different because both electrical resistance[6] and the Hall effect[18] can be observed. These observations are not in contradiction with the above argument because the effects are observed only when the superfluid velocity and vector potential vary with time as is the case in the flux flow state.

Consider the mixed state of a type-II superconductor. According to the Abrikosov theory,[19] flux penetrates the superconductor in the mixed state as a lattice of quantized flux lines or vortices. The circulating superfluid of each vortex produces a magnetic field along the axis of the vortex with total flux $\phi_0=(hc/2\mid e\mid)=(2.06\times10^{-7}$ G cm$^2)$. For electrical resistance and the Hall effect to be observed, it is necessary that the vortices move. Equation (2) still applies but is no longer describing a steady-state situation since both $\mathbf{v}_s$ and $\mathbf{A}$ change in time.

We can use the Ginsburg-Landau current equation

$$\mathbf{j}_s=-(n_s\mid e\mid/2m)[\hbar\nabla\chi+(2\mid e\mid/c)\mathbf{A}],$$

where n_s is the local density of superelectrons and χ is the phase of the Ginsburg-Landau order parameter for electrons to compute $\partial\mathbf{v}_s/\partial t$ by setting $\mathbf{v}_s=\mathbf{j}_s/n_se$. Substituting the resulting expression for $\partial\mathbf{v}_s/\partial t$ into Eq. (2) gives[20]

$$-\hbar\nabla(\partial\chi/\partial t)=2\nabla\mu. \quad (3)$$

The average potential gradient in the superconductor may be obtained from Eq. (3) when $B_{\rm av}$ is everywhere constant in time. In this case the rate at which the phase difference between two points is changing is just 2π times the rate at which vortices pass between the two points.[15,21] Since the vortex density is just $B_{\rm av}/\phi_0$, Eq. (3) reduces to[22]

$$\nabla(\mu_{\rm av}/e)=(\mathbf{v}_L\times\mathbf{B}_{\rm av})/c, \quad (4)$$

where $\mathbf{v}_L$ is the velocity of vortices and $\nabla\mu_{\rm av}$ is the average electrochemical potential gradient. Therefore, as long as one is not concerned with variations on the scale of typical vortex dimensions, a steady electro-

[13] See, for example, H. B. Callen, *Thermodynamics*, (John Wiley & Sons, Inc., New York, 1960).

[14] L. Onsager, Phys. Rev. **37**, 405 (1931); **38**, 2265 (1931).

[15] P. W. Anderson, N. R. Werthamer, and J. M. Luttinger, Phys. Rev. **138**, A1157 (1965).

[16] F. London, *Superfluids* (John Wiley & Sons, Inc., New York, 1950), p. 54; J. M. Luttinger, Phys. Rev. **136**, A1481 (1964); M. J. Stephen, *ibid.* **139**, A197 (1965).

[17] J. M. Luttinger [Phys. Rev. **136**, A1481 (1964)] pointed out the connection between the acceleration equation and the lack of thermoelectric effects in the steady state.

[18] A. K. Niessen and F. A. Staas, Phys. Letters **15**, 26 (1965); W. A. Reed, E. Fawcett, and Y. B. Kim, Phys. Rev. Letters **14**, 790 (1965).

[19] A. A. Abrikosov, Zh. Eksperim. i Teor. Fiz. **32**, 1442 (1957) [English transl.: Soviet Phys.—JETP **5**, 1174 (1957)].

[20] This equation was proposed by P. W. Anderson and A. H. Dayem [Phys. Rev. Letters **13**, 195 (1964)] and derived by Anderson *et al.* (Ref. 15); see also P. W. Anderson, in *Lectures on the Many-Body Problem*, edited by E. R. Caianiello (Academic Press Inc., New York, 1964), pp. 113–135.

[21] G. B. Yntema, Bull. Am. Phys. Soc. **10**, 580 (1965); P. W. Anderson, in *Quantum Fluids*, edited by D. Brewer (North-Holland Publishing Company, Amsterdam, 1966).

[22] This is a special case of the more general equation derived by B. D. Josephson [Phys. Letters **16**, 242 (1965)].

chemical potential gradient exists whenever there is steady vortex motion.

It is indicated both experimentally[6] and theoretically[23–25] that the velocity of a vortex is proportional to the applied force. Neglecting the Hall effect,

$$v_L = \mathbf{F}/\eta, \tag{5}$$

where $\mathbf{F}$ is the force per unit length on a vortex and η is a viscosity coefficient which varies with temperature, maybe with magnetic field but not with velocity.

The force exerted by a transport current may be written[26]

$$\mathbf{F}_j = [\mathbf{j}(H) \times \boldsymbol{\phi}_0]/c. \tag{6}$$

In a magnetically reversible sample (a sample without pinning) having a large demagnetizing coefficient, $j(H)$ is the transport current j (in esu) averaged over a distance large compared to the distance between vortices. For such a sample in the geometry of Fig. 1, combining Eqs. (4)–(6) gives the familiar result

$$\mathbf{j}_{\rm av} = -(c^2\eta/\mathbf{B}\cdot\boldsymbol{\phi}_0)\nabla(\mu_{\rm av}/e).$$

Consider the heat current due to vortex motion. We assume that a transported (or delivered) entropy S_d per flux quantum is associated with a unit length of a moving vortex. S_d is defined such that for vortices moving with velocity $\mathbf{v}_L$, the heat-current density $\mathbf{q}_L$ associated with the motion of vortices is

$$\mathbf{q}_L = (B/\phi_0)\,T S_d \mathbf{v}_L. \tag{7}$$

It is plausible that one can associate a quantity S_d with a moving vortex because a stationary vortex in a type-II superconductor has a core in which the local entropy density is higher than in the surroundings. It is not at all clear, however, how S_d is related to this entropy density variation for fixed vortices or how S_d should be calculated. Using Eq. (4) for $\mathbf{v}_L$ in the geometry of Fig. 1 gives

$$\mathbf{q}_L = -(cTS_d/\phi_0^2)\nabla(\mu_{\rm av}/e)\times\boldsymbol{\phi}_0. \tag{8}$$

This heat current gives rise to the Ettingshausen effect when the vortices are driven by a transport current. It is interesting that the Ettingshausen effect in a superconductor has been observed to be more than a thousand times larger than in a normal metal.

The above discussion indicates that for type-I or type-II superconductors in the flux-flow state there is reason to expect the thermomagnetic effects to be present. Since the mechanism which produces the electrochemical potential is different from that in a normal metal, it is reasonable that the magnitude of the thermomagnetic effects should be quite different from those in the normal metal. In the absence of pinning, the flows and driving forces may be related by a linear expression like Eq. (1) provided the flows and driving forces are averaged over a distance large compared to the size of a vortex. Henceforth, we assume the symbols for flows and forces stand for such average quantities. Including the Hall effect and the thermal force on a vortex gives the following equation for the geometry of Fig. 1 when all electrochemical potential gradients are entirely due to flux flow:

$$\begin{pmatrix} -j_x/e \\ -j_y/e \\ q_x \\ q_y \end{pmatrix} = \begin{pmatrix} L_{11} & L_{12} & 0 & L_{14} \\ -L_{12} & L_{11} & -L_{14} & 0 \\ 0 & L_{14} & L_{33} & L_{34} \\ -L_{14} & 0 & -L_{34} & L_{33} \end{pmatrix} \begin{pmatrix} (1/T)\nabla_x\mu \\ (1/T)\nabla_y\mu \\ \nabla_x(1/T) \\ \nabla_y(1/T) \end{pmatrix}, \tag{9}$$

where

$$L_{11} = (c^2\eta T/B\phi_0 e^2)\cos^2\alpha,$$
$$L_{12} = (c^2\eta T/B\phi_0 e^2)\sin\alpha\cos\alpha,$$
$$L_{14} = -(cT^2 S_d/\phi_0 e),$$
$$L_{33} = T^2\mathcal{K}_p,$$
$$L_{34} = T^2 B\mathcal{K}_p\mathfrak{L}_p.$$

In Eq. (9) $\mathcal{K}_p$ is the isothermal heat conductivity and $\mathfrak{L}_p$ is the Righi-Leduc coefficient[13] (which is not necessarily zero in a superconductor), both measured when the vortices are rigidly pinned. α is the Hall angle. The zeros in the matrix result from the assumption that moving vortices transport heat only parallel to their direction of motion. The generalization to include the Hall effect has been made following Bardeen and Stephen[23] and is accomplished by substituting $v_L\cos\alpha$ for $\mathbf{v}_L$ in Eq. (5) and requiring that $\mathbf{v}_L$ be at the angle α to $\mathbf{F}$ as shown in Fig. 1. The matrix coefficient which relates j_x to $\nabla_y(1/T)$ may be obtained by using the Onsager reciprocity relation $L_{14} = -L_{41}$; a similar procedure is followed for j_y. The coefficient is the same as is obtained by substituting the thermal force on a vortex, $\mathbf{F}_T = -S_d\nabla T$,[27] for $\mathbf{F}$ in Eq. (5).

[23] J. Bardeen and M. J. Stephen, Phys. Rev. **140**, A1197 (1965).

[24] A. G. van Vijfeijken and A. K. Niessen, Philips Res. Rept. **20**, 505 (1965).

[25] P. Nozières and W. F. Vinen, Phil. Mag. **14**, 667 (1966).

[26] This equation was originally suggested by C. J. Gorter, Physica **23**, 45 (1957); Phys. Letters **1**, 69 (1962); P. W. Anderson, Phys. Rev. Letters **9**, 309 (1962). $\mathbf{j}(H)$ was assumed to be the transport current density. Derivations of the equation have been given by J. Friedel, P. G. deGennes, and J. Matricon, Appl Phys. Letters **2**, 119 (1963); G. B. Yntema, in *Proceedings of the Tenth International Conference on Low-Temperature Physics, Moscow, 1966* (Proizvodstrenno-Izdatel'skii Kombinat, VINITI, Moscow, USSR, 1967); Phys. Rev. Letters **18**, 642 (1967); and J. E. Evetts and A. M. Campbell, in *Proceedings of the Tenth International Conference on Low-Temperature Physics, Moscow, 1966* (Proizvodstrenno-Izdatel'skii Kombinat, VINITI, Moscow, USSR, 1967). In these derivations $\mathbf{j}(H)$ is equivalent to $\nabla\times\mathbf{H}(B)$ where $\mathbf{H}(B)$ is the Abrikosov equilibrium field corresponding to the local average induction $B_{\rm av}$. A similar expression was derived by B. D. Josephson, Phys. Rev. **152**, 211 (1966).

[27] This expression was obtained by G. B. Yntema, Phys. Rev. Letters **18**, 642 (1967). A similar expression was obtained by M. J. Stephen (Ref. 10). In Ref. 10, $\phi_0 S/B$ appears for S_d where $\phi_0 S/B$ is the derivative of the free energy per vortex with respect to temperature. It is not clear how $\phi_0 S/B$ is related to S_d as defined by Eq. (7).

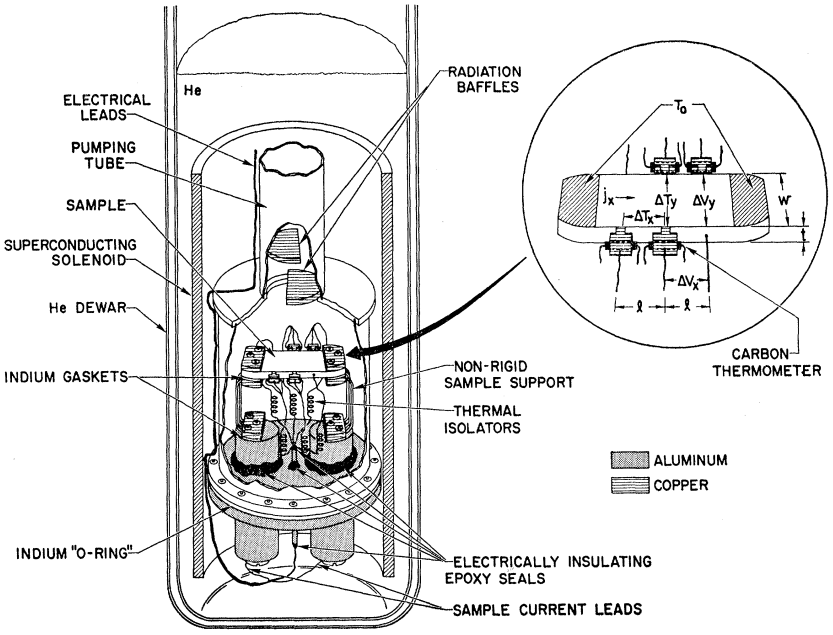

FIG. 2. Experimental apparatus for Ettingshausen- and Nernst-effect measurements.

The thermal force on a vortex F_T may be derived in a simple manner which is similar to the Kelvin derivation of the Kelvin thermoelectric relations. Consider a superconductor in the mixed state operating as a heat engine between two reservoirs at temperatures T and $T-\Delta T$ separated by a distance Δx. The work obtained from the engine when one vortex is allowed to move down the thermal gradient is the thermal force F_T times Δx. The heat supplied by the higher temperature reservoir to the vortex is TS_d. We assume that the normal heat conduction process and the vortex transport of heat are not coupled. Then in principle one can eliminate the dissipative effects, and the engine will have the Carnot efficiency $\Delta T/T$. Then

$$F_T\Delta x/TS_d=\Delta T/T$$

and

$$F_T=S_d(\Delta T/\Delta x)$$

from hot to cold. No thermal force can exist perpendicular to the thermal gradient because such a force would permit extraction of work with no heat transported, in violation of the second law of thermodynamics.

III. EXPERIMENTAL APPARATUS

The measurements of the Ettingshausen and Nernst effects were made in the apparatus shown in Fig. 2. The sample was a thin rectangular slab of superconducting material. It was situated in an evacuated can which was immersed in liquid helium. A magnetic field perpendicular to the broad face of the sample was produced by a superconducting solenoid surrounding the can. To reduce strain, the sample was supported by two nonrigid supports made from strands of copper wire. The nonrigid supports were connected to two aluminum posts which extended through the aluminum base plate of the can. Electrically insulating vacuum seals between the posts and the base plate and between the sample leads and the base plate were made with Emerson and Cuming Stycast 2850 epoxy. The vacuum seal between the can and the base plate was made with an indium O ring. In addition to supporting the sample, the aluminum posts and nonrigid sample supports served as thermal shorts between the ends of the sample and the helium bath. Indium gaskets between the sample and the nonrigid support and between the support and the aluminum posts insured good thermal contact. Electrical current was passed through the sample via the aluminum posts and superconducting niobium-zirconium wires connecting the posts to the sample ends.

Temperature differences along and across the sample were measured by four calibrated carbon resistors which were mounted in copper blocks soldered to the edges of the sample. The resistance of a carbon resistor was measured with an ac Wheatstone bridge. When a measurement of the temperature difference between two resistors was desired, both resistors were used as arms of the bridge. The temperature difference was computed from the resistance ratio. Each thermometer lead included a long section of manganin wire to provide thermal isolation between the thermometers and the helium bath. Leads connected to the edge of the sample were used to measure electrical potential differences along and across the sample. The measurements were made with an Astrodata nanovoltmeter which drove an x-y recorder. Each potential lead included a long coil of very thin copper wire for thermal isolation.

The samples studied were alloys made from 99.999% pure constituents. The constituents were sealed in an

evacuated glass tube. The tube was heated in a rocker furnace to mix the constituents and then quenched in water. To prepare the desired shape, material was first passed through a rolling mill, then squashed to the desired thickness in a hydraulic press, and finally cut with a sharp blade. The most extensively studied samples were a type-II alloy of In+40 at.% Pb (length 3 cm, width 0.5 cm, thickness 0.17 cm) and a type-I alloy of Sn+0.05 at.% In (length 3.5 cm, width 1 cm, thickness 0.05 cm). The type-II alloy was annealed for over one week at 165°C before mounting.

IV. MEASUREMENTS

All the samples which we studied had appreciable pinning forces. In this case the flows and driving forces are not linearly related, and so it is not convenient to use the usual thermomagnetic coefficients. The Ettingshausen coefficient, for example, would depend on the measuring current. When pinning is important, a useful set of parameters to use is η, α, S_d, $\mathcal{K}_p$ and $\mathcal{L}_p$. These coefficients were defined in Sec. II. We must generalize the relationships given by Eq. (9) to include pinning. For simplicity we will assume $\alpha=\mathcal{L}_p=0$ which is a good approximation for the samples studied.

Except for setting α and $\mathcal{L}_p$ equal to zero, the heat-current equations remain unchanged. We use these equations to describe the Ettingshausen effect. Referring to the insert in Fig. 2 the measurement is made by passing current through the sample and measuring the temperature difference ΔT_y and the electrical potential difference ΔV_x. [The meter reading ΔV presumably gives $\Delta(\mu/e)$ between sample probes.] The heat current equation for the y direction is

$$q_y=(cT^2S_d/\phi_0 e)(1/T)\nabla_x\mu+T^2\mathcal{K}_p\nabla_y(1/T). \quad (10)$$

Since no heat enters or leaves the sides of the sample, $q_y=0$. The temperature and potential gradients are uniform and so may be obtained from the measured differences ΔT_y and ΔV_x.[28] $\mathcal{K}_p$ may be measured independently, so we can use Eq. (10) to determine the coefficient S_d from measured quantities:

$$S_d=10^{-8}(\mathcal{K}_p\phi_0 l/Tw)(\Delta T_y/\Delta V_x) \quad (11)$$

where all quantities are in gaussian units except for ΔV_x which has been converted to volts. If S_d is independent of vortex velocity, then ΔT_y is proportional to ΔV_x at a given magnetic field and temperature. Figure 3 shows some Ettingshausen effect data for a type-II alloy. The curves are linear up to several μV.

$\mathcal{K}_p$ was measured by disconnecting one end of the sample from thermal contact with the bath and measuring ΔT_x while supplying a known quantity of heat to the disconnected end. The thermal gradient may be kept small enough so that no vortex motion is produced. Then $\mathcal{K}_p=-\nabla_x T/q_x$. The thermal conductivity was also measured when the heat supplied to the sample was produced by resistive heating in the sample itself. The temperatures at three points along the sample were measured, and the thermal conductivity was computed assuming a parabolic temperature distribution. This method tended to be inaccurate in the superconducting state where inhomogeneities in the sample produced nonuniform heating.

The current density equation in the presence of pinning may be derived by using the applied force minus the pinning force for **F** in Eq. (5). We assume that α and $\mathcal{L}_p$ are zero and that the pinning force is equal and opposite to the applied force when the applied force is less than the critical value for depinning and is constant when the applied force is well above critical. The equation for the x component of force may then be written

$$(j_y\phi_0/c)-S_d\nabla_x T-F_{px}=-(c\eta/Be)\nabla_y\mu,$$

where F_{px} is the x component of the pinning force. To measure the Nernst effect, the electrical currents are set equal to zero. We can see from the above equation that no Nernst voltage will be observed unless the thermal force $-S_d\nabla_x T$ is big enough to overcome the pinning force. We have thus far been unable to achieve this situation. One can, however, reduce the x component of the pinning force by applying an electrical current in the x direction which has the effect of rotating the pinning force toward the y axis. The situation is shown in Fig. 4. If we assume that the maximum value for the pinning force is independent of its direction, then the x component of the pinning force may be made arbitrarily small. It may be seen by comparing the similar triangles in Fig. 4 that

$$\frac{-S_d\nabla_x T}{(j_x\phi_0/c)}=\frac{(c\eta\nabla_y\mu)/Be}{(c\eta\nabla_x\mu)/Be}.$$

This measurement therefore gives the following ex-

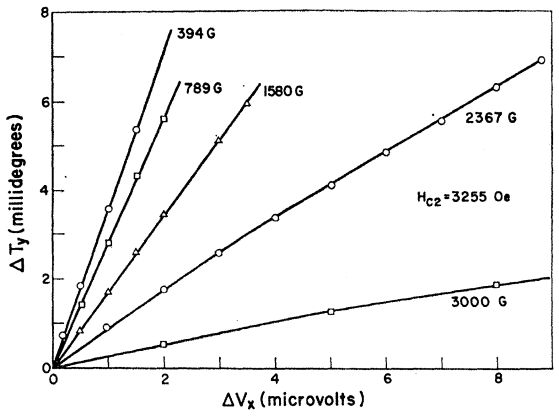

FIG. 3. Ettingshausen temperature difference versus longitudinal potential difference for a type-II alloy (In+40 at.% Pb).

[28] Strictly speaking, this statement and, consequently, Eq. (11), are valid only for a very long sample. Equation (11) is accurate to about 1 % or better for $l/w>3.5$.

pression for S_d:

$$S_d = -\frac{(\Delta V_y/w)}{(\Delta V_x/l)}\frac{j_x\phi_0}{c\nabla_x T}, \tag{12}$$

where j_x is measured in esu. The temperature gradient was provided by the parabolic temperature distribution produced by resistive heating in the sample. $\nabla_x T$ at any point along the sample was calculated from the measured values of ΔT_x.

In Fig. 5 we show how the transverse potential difference ΔV_y varies with current. The observed voltage had a component odd in current which was probably due to probe misalignment and a component even in current which we associate with the Nernst effect. The even component increased with increasing temperature gradient and was always in the expected

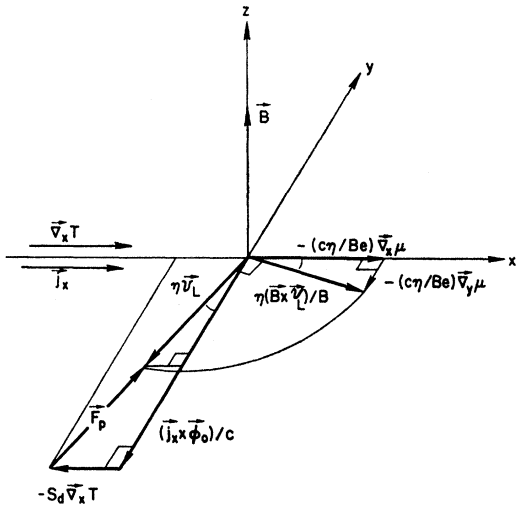

FIG. 4. Forces on a vortex. The figure shows the motion of a vortex which is being driven by a force due to a transport current, a thermal force, and a pinning force. The electric field is rotated 90° from the direction of motion as shown. All vectors are expressed in units of force per unit length of a vortex. The Hall angle is assumed to be zero.

direction for vortices moving from hot to cold. The longitudinal temperature difference ΔT_x (proportional to the temperature gradient at the probes) is also shown in Fig. 5 to demonstrate the correlation with the even component of ΔV_y.

Recently, the Nernst effect was seen in the absence of a transported current in an alloy of Nb with 15 at.% Mo by Lowell *et al.*[5]

V. RESULTS FOR A TYPE-II ALLOY: In+40.0 at.% Pb

The thermal conductivity $\mathcal{K}_p$ was measured as a function of magnetic field at several temperatures. The results for zero magnetic field and a field greater than H_{c2} are plotted in Fig. 6. There is significant variation of the superconducting-state thermal conductivity which is correlated with the condition of anneal of the

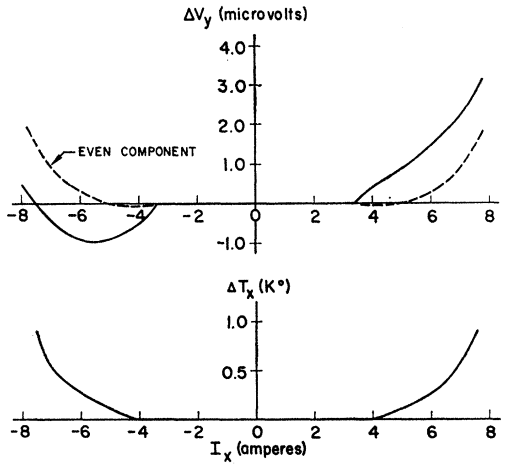

FIG. 5. Nernst effect: transverse potential difference and longitudinal temperature difference versus sample current. The even component of the transverse potential difference is shown, and the expected correlation with the longitudinal temperature difference can be seen.

sample. The thermal conductivity measured after the sample had been slightly cold worked was higher than that measured after the sample had annealed at room temperature for several days. The solid squares in Fig. 6 were measured after a 2-week anneal. This effect seems rather odd and will be the subject of further investigation. For the purpose of this paper this effect is annoying since it adds to the uncertainty in S_d at low magnetic fields.

The quantity S_d was obtained from Ettingshausen-effect measurements. It was computed using the meas-

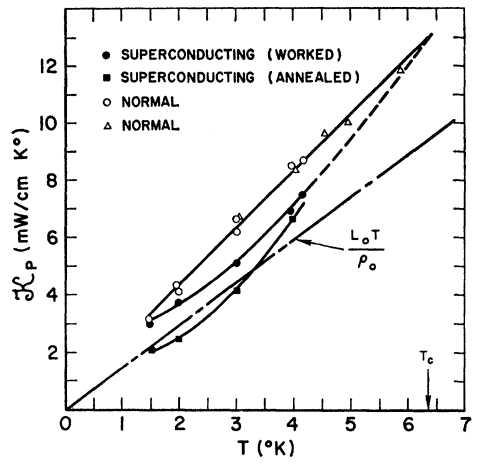

FIG. 6. Thermal conductivity of In+40 at.% Pb in the normal and superconducting states versus temperature. The thermal conductivity in the superconducting state depends on the condition of anneal. The circles are for a slightly cold-worked sample, and the squares are for the same sample after 2 weeks of anneal at room temperature. The condition of anneal does not affect the normal-state thermal conductivity. Also shown is the electronic contribution in the normal state calculated from the Wiedemann-Franz ratio. L_0 is the Lorentz number, and ρ_0 is the measured residual resistivity (16.5 $\mu\Omega$ cm). The triangles were taken with a parabolic temperature distribution. All other points were taken with a linear temperature distribution.

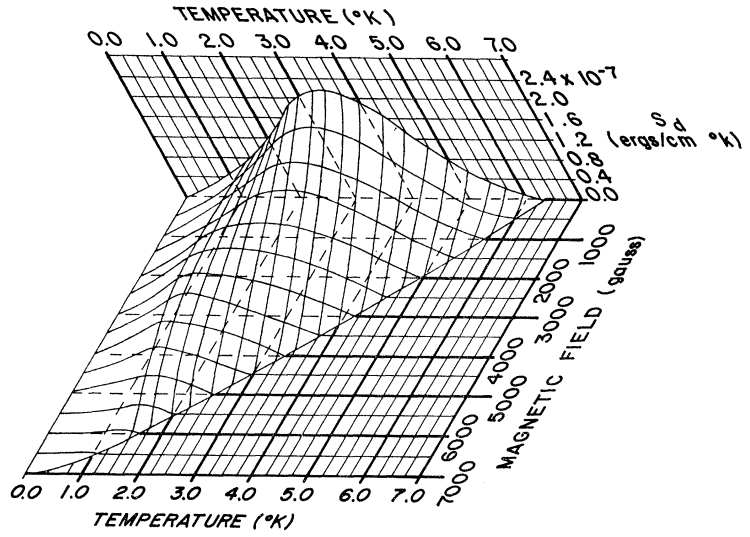

FIG. 7. Three-dimensional plot of S_d versus B and T for In+40 at.% Pb. The surface was constructed to pass smoothly through the Ettingshausen data points and was extrapolated to $T=0$ and $B=0$.

ured values of $\mathcal{K}_p$ and $\Delta T_y/\Delta V_x$ in Eq. (11). The result, shown in Fig. 7, is a surface of S_d as a function of temperature and magnetic field. The surface was constructed to pass smoothly through the data points and was extrapolated to $T=0$ and $B=0$. The surface is least accurate at low temperatures and low magnetic fields where some of the data points may have as much as 50% uncertainty. Part of this uncertainty is due to variations in $\mathcal{K}_p$. Part is due to nonuniform flux flow caused by inhomogeneities in the sample.

The quantity S_d was also obtained from Nernst-effect measurements. It was computed using the measured values of ΔV_x, ΔV_y, j_x, and ΔT_x in Eq. (12). The results are the triangles in Fig. 8, where S_d is plotted as a function of magnetic field for two different temperatures. The uncertainty in these points may be as large as 50%. We have also plotted values of S_d obtained using the Ettingshausen effect (circles). The curves are the intersections of the S_d surface in Fig. 7 with the constant-temperature planes. It should be emphasized that the surface is smoothed over temperature as well as magnetic field. For these two temperatures the surface happens to lie below the experimental points. The figure gives some idea of the deviations of the data points from the S_d surface. That the two methods of obtaining S_d yield similar results is consistent with the Onsager reciprocity relations.

The curves in Fig. 8 are typical of all curves of S_d versus field in having a gradual decrease from a maximum value at low fields to zero at $B=H_{c2}$. This behavior is in accord with our qualitative understanding of the entropy transported by moving vortices. When the vortices are well separated, the formation of a new vortex at the edge of the sample involves a local depression of the order parameter from its BCS value. The electrons in the vicinity of the vortex absorb heat from the lattice to bring them into thermal equilibrium with the lattice. As the vortex is moved, the excitations localized about the vortex[29] will also move. When the vortex is destroyed at the other side of the sample, these localized excitations will dump heat back into the lattice. Absorption of heat on one side and deposition of heat on the other result in a temperature difference whose magnitude is determined by how fast the heat flows back across the sample by ordinary conduction processes. As the density of vortices increases, more excitations become nonlocal because there is a general depression of the order parameter throughout the sample and because some excitations may tunnel from vortex to vortex.[30] This results in a decrease in the entropy transported per vortex.

Another phenomenon which is related to the distinction between local and nonlocal excitations associated with a vortex is the electronic contribution per vortex to the thermal conductivity in the mixed state. The electronic thermal conductivity along the vortex axis will get contributions from both the local and nonlocal excitations while only the nonlocal excitations will contribute to the thermal conductivity perpendicular to the vortex axis. The difference between parallel and perpendicular thermal conductivity per vortex should therefore be related to the density of local excitations. This difference was recently measured in an $In_{0.95}Pb_{0.05}$ alloy by Parks *et al.*[31] Their results indicate that once the sample is in the mixed state, there is a continuous decrease in the difference between parallel and perpendicular thermal conductivity from a maxi-

[29] A discussion of localized excitations connected with a vortex has been given by C. Caroli, P. G. deGennes, and J. Matricon, Phys. Letters **9**, 307 (1964).

[30] E. Canel, Phys. Letters **16**, 101 (1965); D. Markowitz and B. B. Schwartz, in Proceedings of the Conference on the Physics of Type-II Superconductivity, Cleveland, Ohio, P.I.-50 (unpublished); J. Matricon, *ibid.* P.I.-87 (unpublished).

[31] R. D. Parks, F. C. Zumsteg, and J. M. Mochel, Phys. Rev. Letters **18**, 47 (1967).

mum at low fields to zero at $B=H_{c2}$. This is similar to our results for the quantity S_d and is consistent with the ideas presented in the previous paragraph.

Since we do not know how to calculate the effects of overlap, we extrapolate S_d linearly to $B=0$ to compare with the theories for well-separated vortices. The hope is that at low magnetic fields the vortices are well enough separated so that all the excitations associated with vortices are local. The extrapolated points are the circles in Fig. 9. The error bars represent our estimate of the combined uncertainties in the extrapolation to $B=0$, the measurement of the thermal conductivity, and the deviations from linearity of the ΔT_y-versus-ΔV_x curves (at low fields the nonlinearity near the origin was in many cases considerably worse than is shown in Fig. 3 and was probably caused by nonuniform flux flow). The solid line is the intersection of the S_d surface with the $B=0$ plane.

Also shown in Fig. 9 (squares) is the incremental entropy S_i, obtained calorimetrically.[12] S_i is the increment of entropy that must be added to the sample to maintain constant temperature when an additional cm of vortex is added to the sample by increasing the applied magnetic field. S_i includes contributions from both the local and nonlocal excitations and should therefore be larger than S_d at high magnetic fields. This feature is experimentally observed. The values of S_i shown in Fig. 9 were also extrapolated to $B=0$. One may conjecture that if S_d is measured under conditions where the vortices move in complete thermal equilibrium with the lattice and are well enough separated so that all the excitations associated with a vortex are local, then this value of S_d would be the same as the extrapolated value of S_i. As can be seen from Fig. 9, S_i and S_d are not equal. It is possible that at low temperatures the uncertainties in determining S_i and S_d in small magnetic fields (because of the large amount of pinning) may account for the discrepancy. In fact, the experimental errors in the measured S_i are such as to make the measured value smaller than the real value, and correcting S_i would bring it closer to S_d at low

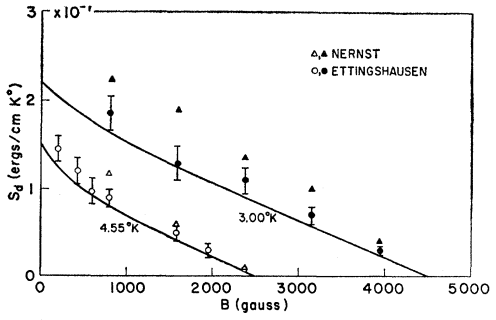

FIG. 8. Magnetic field dependence of S_d for In+40 at.% Pb. The triangles are from the Nernst-effect measurements, and the circles are from the Ettingshausen-effect measurements. The curves are the intersections of the surface of Fig. 7 with the constant-temperature planes.

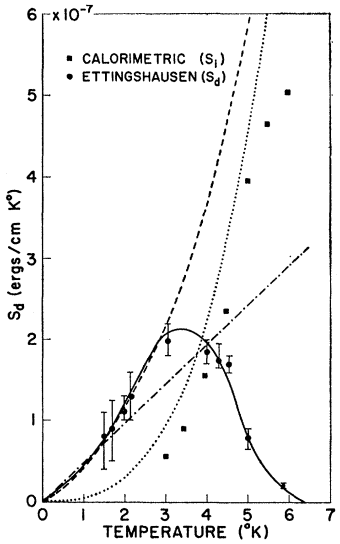

FIG. 9. Temperature dependence of S_d extrapolated to $B=0$ for In+40 at.% Pb. The circles are from the Ettingshausen data and the solid curve comes from Fig. 7. The other curves are calculated from theory as explained in the text. Also shown (squares) is the calorimetrically measured incremental entropy S_i.

temperatures but farther away at high temperatures. The uncertainties in S_i and S_d at high temperature, however, are much too small to account for the difference, and it must be considered real. If we assume the measurement techniques are satisfactory, then either the conjecture that S_i and S_d are equal at low magnetic fields is wrong, or the vortices do not move in thermal equilibrium, or experimentally we have not achieved the condition of well-separated vortices. It is not clear which explanation is correct. As indicated by Fig. 3, the measured value of S_d is independent of the velocity of vortices. This lack of velocity dependence indicates that, if the vortices are not in thermal equilibrium with the lattice, the lack of thermal equilibrium is not dependent on the velocity over a wide range of velocities.

Figure 9 also shows several theoretical estimates of the entropy associated with a unit length of a single quantum vortex in the limit $B=0$. The dot-dash line is calculated from a theory due to van Vijfeijken.[11] He has assumed that the entropy associated with a vortex is the entropy increase necessary to produce a normal core. The dotted curve and the dashed curve are calculated from the theory of Stephen.[10] He has calculated the entropy per vortex by differentiating with respect to temperature the expression for the free energy of a mixed-state superconductor just above H_{c1}. This expression is the sum of a term involving the derivative of the penetration depth with respect to temperature and a term involving the derivative of κ_3 with respect to temperature. The dashed curve is the sum of these two terms using Stephen's approximation for the latter.

The dotted curve is Stephen's high-temperature approximation. It should be pointed out that while the theories are presented by their authors as estimates of S_d, they are really estimates of S_i. As can be seen from Fig. 9, at high temperatures (where the discrepancy between S_i and S_d is most firmly established) the theoretical curves agree better with S_i than with S_d.

VI. RESULTS FOR A TYPE-I ALLOY: Sn+0.05 at.% In

The thermal conductivity of Sn+0.05 at.% In in the normal and superconducting states is shown in Fig. 10. Also shown is the electronic contribution to the thermal conductivity predicted from the Wiedemann-Franz ratio. The thermal conductivity is largely electronic. There is excellent agreement between the experimental shape of $\mathcal{K}_p(B\to 0)/\mathcal{K}_p(B\to H_c)$ versus T and the theoretical prediction of Bardeen, Rickayzen, and Tewordt[32] for electronic conduction limited by impurity scattering. The measured field dependence of $\mathcal{K}_p(B)$ at various temperatures is given approximately by the relation

$$[\mathcal{K}_p(B)-\mathcal{K}_p(B\to 0)]/[\mathcal{K}_p(B\to H_c)-\mathcal{K}_p(B\to 0)]=h^3,$$

where $h\equiv H/H_c$. The critical-field curve of the alloy is almost that of pure Sn ($H_0=305$ Oe and $T_c=3.66$°K).

The demagnetizing factor for slabs used in our experiments is very close to one, and a type-I sample goes into the intermediate state at very low fields ($h<0.04$). An experiment on magnetic coupling between two closely adjacent slab-shaped samples[7] indicates that the potential difference across a current-carrying type-I slab in the intermediate state results from both vortex flow[33] and the resistance of normal regions which interrupt the superconducting paths. The experiment was performed with a sandwich of two superconducting strips (called the primary and secondary) separated by a thin insulating layer. A magnetic field was applied perpendicular to the broad face of the sample, and a current was passed through the primary. If the current-produced vortex motion across the primary and the two superconductors were in close enough proximity, then vortices were also pulled across the secondary. The simultaneous motion of vortices was evidenced by a potential difference which appeared between the ends of the secondary whenever one appeared between the ends of the primary. At low magnetic fields the ratio of secondary to primary potential differences, which we call the coupling parameter, was close to 1, indicating that flux flow was the major contributor to the primary potential difference. At an intermediate field H_α (H_α is about 0.5 H_c in Sn), the coupling parameter, fell rapidly to zero. This behavior was observed in samples having insulators as thin as 1000 Å and as thick as 20 000 Å. This would be explained by assuming that the decrease in the coupling parameter is caused by the disappearance of flux flow as the resistance mechanism. If this is so, then the coupling parameter is simply equal to the fraction $f(B)$ of the potential difference across the primary which is due to flux motion; the fraction $1-f(B)$ is presumably due to the resistance of normal regions. Observations of the patterns produced by a diamagnetic powder sprinkled on a sample in the intermediate state at fields close to H_c substantiate the hypothesis.[34] The observations show alternating normal and superconducting lamina oriented perpendicular to the direction of electrical current. For such a topology the potential difference would be entirely due to the resistance of the normal regions.

The measurements of van Gurp[8] also indicate a decrease in $f(B)$ with increasing magnetic field. He has measured the noise voltage of a type-I slab in the resistive intermediate state. He observed noise associated with flux flow at low magnetic fields but no such noise at high magnetic fields.

If above H_α flux flow is not the major mechanism for electrical resistance, then the Ettingshausen effect should also be small, since the Ettingshausen temperature difference in the absence of flux flow is significantly smaller than in the presence of flux flow. Figure 11 shows the experimental results. The points are experimental values of $f(B)$ times S_d. This quantity is determined from Eq. (11) which has been modified to include the possibility that only part of the observed potential difference is due to flux flow. One simply replaces ΔV_x by $f(B)\Delta V_x$ and transposes the unknown quantity $f(B)$ to the left-hand side of the equation. The solid curves represent the coupling parameter for pure Sn normalized to the zero-field intercept of $f(B)S_d$. At low temperatures $f(B)S_d$ follows the

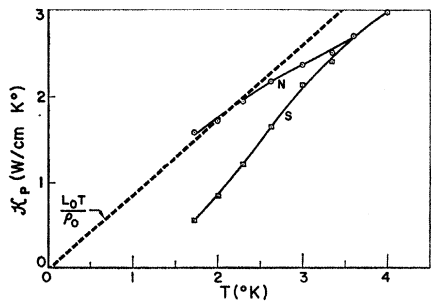

FIG. 10. Thermal conductivity of Sn+0.05 at.% In in the normal and superconducting states versus temperature. Also shown is the normal-state electronic contribution predicted from the Wiedemann-Franz ratio. L_0 is the Lorentz number, and ρ_0 is the measured residual resistivity, 2.8×10^{-8} Ω cm.

[32] J. Bardeen, G. Rickayzen, and L. Tewordt, Phys. Rev. **113**, 982 (1959); G. Rickayzen, *Theory of Superconductivity* (Interscience Publishers, Inc., New York, 1965), p. 277.

[33] By vortex in a type-I sample, we mean a normal spot completely surrounded by a superconducting region. Such a vortex may be large and contain many flux quanta.

[34] P. R. Solomon and F. A. Otter, Jr., in Proceedings of the Conference on Transport Properties of Superconductors, University of Kent, 1967 (unpublished); P. R. Solomon (to be published).

coupling curves very well. This is good evidence that both curves reflect the shape of $f(B)$. At higher temperatures $f(B)\,S_d$ starts dropping at lower fields than does the coupling parameter. This may reflect a drop in S_d possibly because of overlap effects. Finally, there is some persistence of $f(B)\,S_d$ [or ΔT(Ettingshausen)] above H_α. Experiments with powder patterns seemed to show some motion of domain walls (not vortex motion) which may explain this effect.[34]

We extrapolate $f(B)\,S_d$ to $B=0$, where no overlap effects are expected and where $f(B)$ can be set equal to 1 as indicated from the coupling experiments. These results are displayed in Fig. 12. The error bars are large because of the large amount of pinning at low fields, and the resultant temperature dependence of S_d at $B=0$ is not completely clear. A simple model for well-separated vortices (which is similar to van

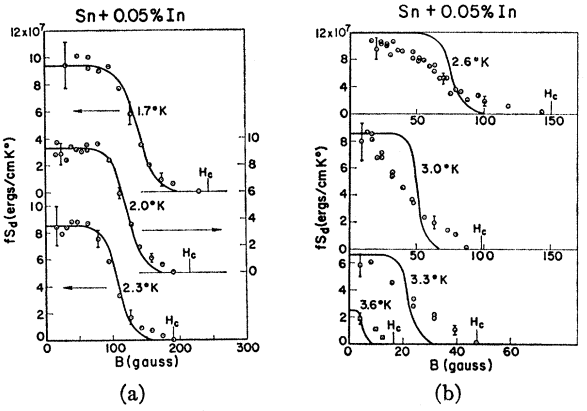

FIG. 11. Magnetic field dependence of $f(B)\,S_d$ for Sn+0.05 at.% In. The points are from Ettingshausen-effect measurements. The curves represent the coupling parameter of Ref. 7 normalized to the zero-field intercept of $f(B)\,S_d$. Also shown are representative error bars.

Vijfeijken's model)[11] predicts a linear dependence on T, and the result is shown for this alloy as the straight line in Fig. 12. According to this model, a vortex is a normal spot with sharply defined boundaries having $B=H_c$ inside and zero outside. S_d is simply the entropy per unit length of a vortex divided by the number of flux quanta:

$$S_d = A\Delta S_{n-s}/(H_c A/\phi_0), \tag{13}$$

where A is the cross-sectional area of the vortex and ΔS_{n-s} is the entropy difference per unit volume between the normal and superconducting states. ΔS_{n-s} may be written

$$\Delta S_{n-s} = S_n - S_s = -(1/4\pi)H_c(dH_c/dT). \tag{14}$$

Assuming H_c is parabolic in T and substituting Eq. (14) into Eq. (13), we get

$$S_d = ((\phi_0 H_0)/(2\pi T_c^2))T. \tag{15}$$

While the experimental and theoretical results agree roughly at low temperatures, the agreement is poor near

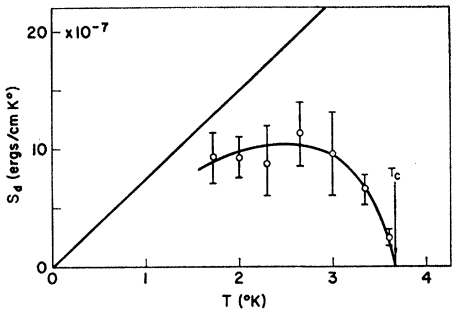

FIG. 12. Temperature dependence of S_d extrapolated to $B=0$ for Sn+0.05 at.% In. The straight line represents the model described in Sec. VI. The error bars include errors in extrapolations to $B=0$.

T_c. It is not yet understood whether the lack of agreement near T_c occurs because the model fails or because the extrapolation to $B=0$ is incorrect. Overlap effects or failure of vortices to move in thermal equilibrium with the lattice might cause an incorrect extrapolation.

Figure 13 shows a three-dimensional view of $f(B)\,S_d$ versus magnetic field and temperature for the type-I alloy. The region below 1.5°K is assumed to be linear in T in accord with the above model. Except for the already discussed sudden drop at H_α, the surface looks very similar to that for a type-II superconductor. This similarity may indicate that the mechanism for the drop to zero of S_d near T_c is common to all superconductors.

VII. CONCLUSIONS

We have demonstrated the existence of the Ettingshausen and Nernst effects in the presence of vortex flow in superconductors. These and other thermomagnetic effects are discussed in terms of a simple phenomenological theory which contains the parameter S_d, the transport entropy (per cm per quantum of flux) of a moving vortex. Measurements of S_d for a type-I (Sn+0.05 at.% In) and a type-II (In+40 at.% Pb) alloy are presented. At vanishing field, S_d first increases with temperature and then returns to zero at T_c. Simple models give reasonable estimates of S_d at low

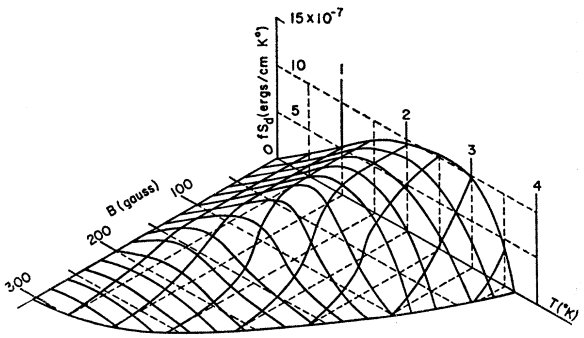

FIG. 13. Three-dimensional plot of $f(B)\,S_d$ for Sn+0.05 at.% In.

temperatures but fail to account for the return to zero at T_c. At fixed temperature, S_d for a type-II superconductor decreases monotonically from the low-field value to zero at H_{c2}. This result is interpreted to be a consequence of increasing overlap of vortices. In type-I superconductors, S_d is also zero at the critical field H_c but in contrast with type-II superconductors, the magnitude of the Ettingshausen effect at low fixed temperatures drops abruptly at about 0.5 H_c. The sudden drop in the magnitude of the Ettingshausen effect is consistent with the previously suggested hypothesis[7] that the mechanism of resistance in a current-carrying intermediate-state slab changes from vortex flow to some other resistive mechanism, such as normal regions, which interrupt the superconducting paths.

Measurements of S_d for a barely type-II superconductor (Nb) are in progress. Experiments bearing on the question of why S_d returns to zero at T_c are planned.

ACKNOWLEDGMENTS

The authors have had numerous helpful discussions with B. Burdick, J. B. Burnham, R. E. Hodder, G. A. Peterson, M. P. Shaw, M. J. Stephen, and G. B. Yntema, who has been especially helpful. Thanks are due J. B. Burnham for much of the data taking and R. Siegmund and C. Ward for other experimental assistance.

PHYSICAL REVIEW VOLUME 164, NUMBER 2 10 DECEMBER 1967

Anomalies in the Magnetic Field Dependence of the Surface Impedance of Superconducting Sn†

J. F. KOCH AND C. C. KUO

Department of Physics and Astronomy, University of Maryland, College Park, Maryland

(Received 12 June 1967)

We have made an extensive study of the microwave surface resistance of superconducting Sn as a function of magnetic field. At reduced temperatures $t \gtrsim 0.6$ and microwave frequencies in the range of 28 to 56 Gc/sec, we find some unusual peaks in the absorption derivative. The anomalous peaks appear at the onset of a range of magnetic field where the resistance decreases with increasing field. The position in field for such a peak is found to vary with temperature approximately as $(1-t^4)^{1/3}$. The amplitude diminishes rapidly with decreasing temperature. The peak position depends linearly on the microwave frequency. The effect is anisotropic with respect to the orientation of the magnetic field in a given sample plane, as well as with the choice of sample plane for a given orientation of the field. The amplitude of the peaks depends on the polarization of the rf current relative to the magnetic field. A very light etching of the sample surface destroys the signals.

The effect is interpreted in terms of magnetic-field-induced surface bound states that correspond to classical skipping orbit trajectories. Such states are shown to have energies in the gap of the energy spectrum of the superconductor. Transitions between the bound state and the continuum above the energy gap can satisfactorily account for the experimental observations. Indeed, we believe that the experiments provide evidence for the existence of surface states in the presence of a magnetic field.

I. INTRODUCTION

MANY metals, including Sn, show an oscillatory variation of the normal-state microwave surface impedance with applied magnetic field in the range 0–100 Oe. This oscillatory effect in the weak-field regime is known to arise from transitions between quantum-mechanical surface states that correspond to classical electron trajectories skipping along the surface. Electrons in such trajectories are bound to the surface region by the magnetic field and perform a periodic motion normal to the metal surface. As Nee and Prange[1] have shown, the quantum-mechanical treatment of this periodic motion leads to a discrete-energy-level spectrum for such electron states.

The observation of some oscillatory variation in the surface impedance of metals in the normal state was first reported by Khaikin[2] and has recently been considered in a detailed study by the authors.[3,4]

The skipping electron trajectories responsible for the oscillations in the normal-state impedance penetrate the metal only to a very small depth. The ground state of the energy-level spectrum corresponds to a penetration into the metal of about 10^{-5} cm, or about one microwave skin depth δ. Successively higher energy

† Research supported in part by the Advanced Research Projects Agency under Grant No. SD-101.

[1] T. W. Nee and R. E. Prange, University of Maryland, Department of Physics and Astronomy, Technical Report No. 668 (unpublished); Phys. Letters (to be published).

[2] M. S. Khaikin, Zh. Eksperim i Teor. Fiz. **39**, 212 (1960) [English transl.: Soviet Phys.—JETP **39**, 152 (1961)].

[3] J. F. Koch and A. F. Kip, in *Low Temperature Physics—LT9*, edited by J. G. Daunt, D. O. Edwards, F. J. Milford, and M. Yaqub (Plenum Press, Inc., New York, 1964), pp. 818–822.

[4] J. F. Koch and C. C. Kuo, Phys. Rev. **143**, 470 (1966).